

Demystifying Platform Requirements for Diverse LLM Inference Use Cases

Abhimanyu Bambhaniya*, Ritik Raj*, Geonhwa Jeong*, Souvik Kundu†, Sudarshan Srinivasan†, Midhilesh Elavazhagan†, Madhu Kumar†, Tushar Krishna*

*Georgia Institute of Technology

†Intel Labs

abambhaniya3@gatech.edu

Abstract—Large language models (LLMs) have shown remarkable performance across a wide range of applications, often outperforming human experts. However, deploying these parameter-heavy models efficiently for diverse inference use cases requires carefully designed hardware platforms with ample computing, memory, and network resources. With LLM deployment scenarios and models evolving at breakneck speed, the hardware requirements to meet SLOs remains an open research question. In this work, we present an analytical tool, GenZ, to study the relationship between LLM inference performance and various platform design parameters. Our analysis provides insights into configuring platforms for different LLM workloads and use cases. We quantify the platform requirements to support SOTA LLMs under diverse serving settings. Furthermore, we project the hardware capabilities needed to enable future LLMs potentially exceeding hundreds of trillions of parameters. The trends and insights derived from GenZ can guide AI engineers deploying LLMs as well as computer architects designing next-generation hardware accelerators and platforms. Ultimately, this work sheds light on the platform design considerations for unlocking the full potential of large language models across a spectrum of applications. The source code is available at [GitHub](#).

I. INTRODUCTION

Large Language Models (LLMs) are among the most popular variants of generative AI models performing autoregressive tasks. LLMs are used in various applications, including chatbots, code generation, question answering, chemical property prediction [79], protein sequencing [49], and video generation [30], [93]. Commercial products like ChatGPT [54], Gemini [69], Claude [45], Github Copilot [104], have performed astonishingly well in diverse metrics, often outperforming human experts [115]. LLMs have shown great scaling law property [52], [88], with larger models [45], [50], [59] demonstrating better performance as compared to the smaller ones [125]. Currently, the largest model is known to have $\sim 1.8T$ parameters [29], with future LLMs potentially exceeding even a few hundred trillion parameters.

LLM inference can be broken into two stages, namely the *prefill* and the *decode* stage. The prefill stage consists of a single forward pass using all the input tokens. The autoregressive decode stage generates one output token with each forward pass of the model. The prefill stage often portrays characteristics similar to training forward pass and has significant computing requirements. In contrast, the decode stage

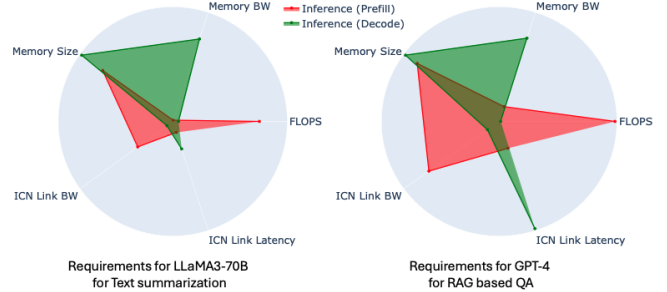


Fig. 1: Summary of platform requirements for two workloads.

requires memory bandwidth and capacity (especially when processing long context queries).

To provide efficient LLM inference, extensive efforts are being made to develop optimizations from both the industry and academic community, including model compression (quantization [68], [86], [129], tensor decomposition [92], pruning [47], [66], [83], knowledge distillation [70], [75]), fast token decoding [57], [64], [67], [91]), system optimizations (paged attention [96], flash attention [61], chunked inference [76], scheduling [130]), and so on. Many of these techniques have also become part of the inference-serving engine such as TensorRT-LLM [105], vLLM [96], DeepSpeed-FastGen [76], and inference servers such as RayLLM [28] with RayServe, TGI [31] and TensorRT-LLM + Triton [39].

The aforementioned works have enabled vast inference performance improvements for LLMs on *current hardware platforms*¹. Unfortunately, they do not automatically provide an answer to how to design *next-generation platforms* for LLM inference. It is not trivial as there are a plethora of emerging LLMs with increasing accuracy and context lengths [133], a diverse suite of LLM inference use cases, and various AI platform vendors (e.g., NVIDIA, Intel, AMD, Google, Cerebras, and others) with their own HW/SW frameworks.

The aim of this work is to demystify and quantify AI platform requirements (i.e., compute FLOPs, memory capacity, memory bandwidth, interconnect latency, and interconnect bandwidth) across a suite of LLM inference use cases and

¹We define platform as the complete hardware back-end including NPUs (e.g., GPUs or TPUs), local memories (e.g. HBM), remote offload memories (e.g., CPU DRAM) and inter-NPU interconnect (e.g., NVlinks/XeLinks).

representative models. To this end, we introduce a first-order analytical model, namely GenZ (Generative LLM analyZer), to distill down the impact of different hardware parameters on end-to-end inference performance. Using this tool, we can study current platforms via efficiency factors for the hardware components (which we determine from real-system validation measurements) without getting limited by their specific software tool chains. We also use GenZ to quantify the hardware requirements for different LLM use cases. These studies help us gain first-order vendor-agnostic insights into platform design and configurations.

To the best of our knowledge, this is the first work to quantify platform-wide requirements for meeting the serving SLOs of generative AI models for different use cases. We believe this work makes two unique contributions to the community. First, the data provided by this work can potentially guide AI engineers working on deploying LLMs to choose suitable hardware platform configurations for their use case(s). Next, this work provides concrete directions to computer architects designing the next generation of AI platforms by navigating the interplay between various HW characteristics and LLM inference performance.

Fig. 1 highlights a subset of our key observations for two distinct deployment scenarios. We have quantified and noticed a significant difference in the serving requirements between the prefill and decode stages. Although the absolute values fluctuate with the workload, the identified trend remains consistent. We identify FLOPS and interconnect BW as the bottleneck for the prefill stage, while memory BW and interconnect link latency are the key bottlenecks for the decode stage.

To summarize, this work makes the following contributions:

- We introduce GenZ, a first-order analytical tool that helps analyze LLM workload on different platforms. Fig. 2 shows an overview of our proposed tool.
- We provide an analysis of the performance impact of different workload optimizations using GenZ.
- We provide an analysis of the performance impact of different platform characteristics using GenZ.
- We provide an analysis of the platform requirements for the target LLM inference to meet the given Service Level Objectives (SLOs) with the target use case using GenZ.

II. KEY TAKEAWAYS

Following are the key takeaways from our work. For detailed understanding please read the rest of the paper. You can also use our code to regenerate the results.

- The prefill and decode stages of the LLM inference process have significant differences in their workloads.
- We find that **increasing** the TFLOPS and inter-chip bandwidth reduces the **prefill** latency but doesn't impact the decoding latency.
- On the other hand, **increasing** the high-speed memory bandwidth(HBM) and reducing the inter-chip network link latency helps improve the latency of the **decode** stage but does not reduce the latency of the prefill stage.

- We also find that for larger systems parallelism plays a major role, where in the **prefill** stage, using **pipeline parallelism** gives the best throughput. During the **decode** stage, a mix of tensor and pipeline parallelism is optimal for throughput in large systems and **tensor parallel** for smaller systems. .
- We also quantify the requirements for meeting the SLO throughput requirements of various models with various use cases and provide analytical formulas to modify the demand according to the usecase and model changes.

III. BACKGROUND

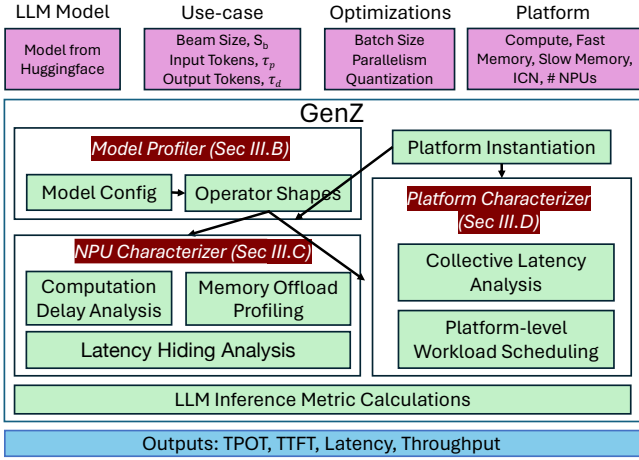
A. LLM Architecture

LLMs are generally designed by stacking multiple transformer decoder layers [124] as shown in Fig. 3. Each layer includes a multi-head self-attention (MHA) and a multi-layer perception (MLP). The key model parameters mainly include the model embedding dimensions (D_{model}), the number of heads (H), the feed-forward hidden dimension (D_{ff}), where D_{ff} is $W_{ff} * D_{model}$, and the number of decoder blocks/layers (L).

For each decoder layer, the input sequence is projected to three linear blocks generating three activations, namely 'Query (Q)', 'Key (K)', and 'Value (V)'. The Q/K/V values are then split into H chunks each of width d, where $d = D_{model}/H$ that can be computed in parallel. For LLMs with group query attention (GQA), H_{kv} chunks of K/V are generated, and these chunks are shared by Q in $\frac{H}{H_{KV}}$ heads. For each attention head, corresponding Q and K are fed to a batch matrix multiplication operation that is then scaled and passed through a softmax operation to compute attention scores. The attention score is multiplied with the V chunk, generating output activations that are then projected via another linear layer. The output of MHA is added to the input of MHA and normalized.

The MLP module consists of three linear layers. FF_{up} , and FF_{gate} projects the input from D_{model} to the higher intermediate dimension D_{ff} . The output of FF_{gate} is activated using non-linear operation. This activation matrix is multiplied with the output of FF_{up} using an element-wise multiplication. FF_{down} projects the output of element-wise multiplication back to D_{model} . The output of MLP is added to the input of MLP and normalized. The final normalized value becomes the input to the decoder layer.

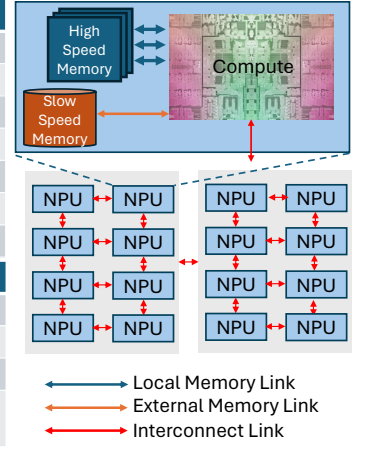
Mixture of Experts (MoE) [65] are special class of LLMs that consist of multiple "expert" multi-layer perceptron (MLP) layers, denoted as 'E', out of which 'K' experts are selected for each input token. In contrast, dense language models can be considered as a special case of MoEs, where $E = K = 1$, meaning there is only one expert MLP layer, and it is used for every input token. By introducing multiple experts and selectively activating a subset of them for each token, MoEs can effectively scale model capacity while maintaining efficient computation and memory usage, making them a promising approach for building larger and more capable language models. Some popular MoE models are Switch



(a) GenZ Overview

Workload		Knobs
LLM Model		Model Name
Use case configs	Beam Size	S_b
	Input Tokens	τ_p
	Output Tokens	τ_d
Optimization Configs	Batch Size	B
	Parallelism	TP / PP
	Quantization	FP8 / Int8 / BF16.
Config.	Knobs	
Compute	FLOPS, Eff_c	
Fast Memory	BW_{fmem} , Cap_{fmem} , Eff_{fmem}	
Slow Memory	BW_{smem} , Cap_{smem} , Eff_{smem}	
Interconnect Network (ICN)	T_{link} , BW_{link} , Eff_{link}	

(b) Configuration Knobs for GenZ



(c) Platform Architecture Abstraction

Fig. 2: An overview of GenZ framework.

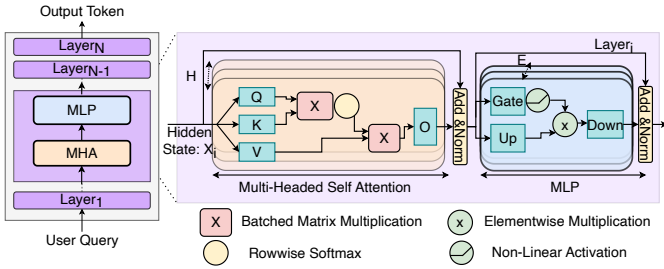


Fig. 3: Typical LLM Model Architecture. Each Layer has multiple parallel heads. For MoE models, there are multiple parallel MLP layers out of which ‘k’ are activated.

Model	D_{model}	Layers	Heads (H_{kv})	W_{ff}	Experts (Selected)
LLaMA2-7B [123]	4096	32	32	~ 2.7	-
Mixtral-8x7B [85]	4096	32	32(8)	3.5	8(2)
LLaMA3-70B [20]	8192	80	64(8)	3.5	-
GPT3-175B [50]	12288	96	96	4	-
GPT4-1.8T [41]	10752	120	84	4	16(2)
Super LLM-10T	13824	128	108	4	32(4)

TABLE I: Different LLM architecture evaluated in this work.

Transformers [65], Mixtral 8x7B [85], Mixtral 8x22B [22], DBRX [5], GROK [11], GPT-4 [9], [10], [41]. Table I presents some of the state-of-the-art LLMs and associated dimensions.

B. Generative LLM Inference

Prefill. The prefill stage runs only once on input sequence of τ_p tokens to generate the K and V activations, which are often kept as the KV cache, for each LLM layer. The generated KV cache would be used for all subsequent output token generation. Table II shows the operator wise breakdown of each LLM decode layer during the prefill stage. C_{op} and M_{op} is the number of floating point calculations, memory requirement required for the operator. The prefill stage is **mostly compute-bounded** as all input tokens can be processed in parallel.

Decode. After the prefill stage, output tokens are generated auto-regressively, i.e. the last generated token is fed as an input to the LLM in each iteration, and one new output ‘token’ is generated. Table III shows the operator-wise breakdown of each LLM decode layer during the decode stage. C_{op} and M_{op} is the number of floating point calculations, memory requirement required for the operator. All the model weights and past KV cache are used to generate a single output token. Since input to the model is a single token, all matrix-matrix multiplications are converted into matrix-vector multiplications. This makes the generation stage **highly memory-bounded**. At the end of each generation step, the newly generated KV cache is padded to the existing KV cache, meaning its linear growth with the output sequence length. Generation stops when a special $\langle end-token \rangle$ is generated, or the user limits the maximum number of output tokens. We define τ_d tokens are generated during the decode phase.

Beam search [77], [89], [103], [121] is a heuristic search algorithm commonly employed in LLMs during the decode stage by recent LLMs. It helps generate more contextually relevant and coherent sequences of words by exploring multiple potential sequences simultaneously. The number of maximum parallel sequences is a user-defined parameter called Beam Size, S_b . Typically $S_b = 4$ for generative inference. During generative LLM inference, the model predicts the next word based on previous context with beam search maintaining a limited set of the likely candidate sequences. These candidate sequences are ranked by their likelihood, and the algorithm continually refines them by considering alternative word choices. By exploring a predefined number of possibilities in parallel, beam search enhances the quality of the generated text. After the common prefill stage, two parallel beams are launched during the decode phase. The beam with the highest likelihood is selected as the final output.

Operation	Input Shapes	Output Shape	C_{op}	M_{op}
$Q/K/V$	$[B, \tau_p, D_{model}] \times [D_{model}, 3D_{model}]$	$3B, \tau_p, H, d$	$O(3B\tau_p D_{model}^2)$	$O(4B\tau_p D_{model} + 3D_{model}^2)$
$Q * K^T$	$[B, \tau_p, H, d] \times [B, \tau_p, H, d]$	B, H, τ_p, τ_p	$O(BH\tau_p^2 d)$	$O(2B\tau_p D_{model} + BH\tau_p^2)$
$P * V$	$[B, \tau_p, \tau_p] \times [B, \tau_p, H, d]$	B, H, τ_p, d	$O(BH\tau_p^2 d)$	$O(2B\tau_p D_{model} + BH\tau_p^2)$
$A * W_O$	$[B, \tau_p, D_{model}] \times [D_{model}, D_{model}]$	B, τ_p, D_{model}	$O(B\tau_p D_{model}^2)$	$O(B\tau_p D_{model} + D_{model}^2)$
FF_{up}	$[B, \tau_p, D_{model}] \times [D_{model}, D_{ff}]$	B, τ_p, D_{ff}	$O(B\tau_p D_{model} D_{ff})$	$O(B\tau_p D_{model} + D_{model} D_{ff} + B\tau_p D_{ff})$
FF_{gate}	$[B, \tau_p, D_{model}] \times [D_{model}, D_{ff}]$	B, τ_p, D_{ff}	$O(B\tau_p D_{model} D_{ff})$	$O(B\tau_p D_{model} + D_{model} D_{ff} + B\tau_p D_{ff})$
FF_{down}	$[B, \tau_p, D_{ff}] \times [D_{ff}, D_{model}]$	B, τ_p, D_{model}	$O(B\tau_p D_{model} D_{ff})$	$O(B\tau_p D_{ff} + D_{ff} D_{model} + B\tau_p D_{model})$

TABLE II: Matrix Multiplication operations during the **prefill** stage. Reduction dimensions are underscored. Blue colored operators are model weights.

Operation	Input Shapes	Output Shape	C_{op}	M_{op}
$Q/K/V$	$[B, 1, D_{model}] \times [D_{model}, 3D_{model}]$	$B, H, 1, d$	$O(3BD_{model}^2)$	$O(3D_{model}^2)$
$Q * K^T$	$[B, 1, H, d] \times [B, \tau_{cur} + 1, H, d]$	$B, H, 1, \tau_{cur} + 1$	$O(BH(\tau_{cur} + 1)d)$	$O(B\tau_{cur} D_{model})$
$P * V$	$[B, 1, \tau_{cur} + 1] \times [B, \tau_{cur} + 1, H, d]$	$B, H, 1, d$	$O(BH(\tau_{cur} + 1)d)$	$O(B\tau_{cur} D_{model})$
$A * W_O$	$[B, 1, D_{model}] \times [D_{model}, D_{model}]$	$B, 1, D_{model}$	$O(BD_{model})$	$O(D_{model}^2)$
FF_{up}	$[B, 1, D_{model}] \times [D_{model}, D_{ff}]$	$B, 1, D_{ff}$	$O(BD_{ff} D_{model})$	$O(D_{ff} D_{model})$
FF_{gate}	$[B, 1, D_{model}] \times [D_{model}, D_{ff}]$	$B, 1, D_{ff}$	$O(BD_{ff} D_{model})$	$O(D_{ff} D_{model})$
FF_{down}	$[B, 1, D_{ff}] \times [D_{ff}, D_{model}]$	$B, 1, D_{model}$	$O(BD_{ff} D_{model})$	$O(D_{ff} D_{model})$

TABLE III: Matrix Multiplication operations during the **decode** stage. Reduction dimensions are underscored. Blue and red colored operators are model weights and KV caches respectively. τ_{cur} is sum of prefill tokens(τ_p) and token generated by LLM before the current token.

C. Retrieval Augmented Generation

Despite the promise of being an exciting paradigm towards Artificial General Intelligence (AGI), LLMs still suffer from the obstacles of factual hallucination [53], [71], [84], [112], incomplete, outdated or incorrect knowledge [73], and the lack of domain-specific knowledge [100], [118]. Enhancing LLMs with external knowledge through Retrieval Augmented Generation (RAG) has been proven effective against all such challenges [48], [72], [80], [97] as mentioned in [56].

Before prefill, RAG takes an input query embedding, compares it against a large vector database using KNN search, and augments the query with the k most similar vectors retrieved from the database. As the size of these knowledge databases can be of the order of trillions [48], several ANN (approximate nearest neighbor) techniques including IVF-PQ [82], HNSW [102], SONG [134], and CAGRA [106] have been proposed over the years that trade-off search latency and memory footprint with recall accuracy. **The key implication of using RAG in LLM serving is a significant increase in the input prompt size. This results in higher Time Per Output Token (TPOT) and larger KV caches.** We study these implications in detail in Section VII.

D. Metrics for LLM Serving

The key metrics for LLM inference serving [42] are:

- 1) **Time To First Token (T_{TFFT}):** Time to complete one forward pass with entire input, τ_p , and generate one output token.
- 2) **Time Per Output Token (T_{TPOT}):** Time to generate an output token for each request. Consecutive tokens would have a time that is nearly identical to token generation. T_{TPOT} for i^{th} output token is proportional to the model weights and $\tau_p + i$.
- 3) **Latency (T_{lat}):** The overall time it takes for the model to generate the full response for a user. Overall response

latency can be calculated using the previous two metrics:

$$T_{lat} = T_{TFFT} + T_{TPOT} \times \tau_d.$$

- 4) **Throughput (μ_{thr}):** Refers to the number of output tokens per second an inference platform can generate over a batch size of B . $\mu_{thr} = B / T_{TPOT}$.

IV. GENZ : GENERATIVE LLM ANALYZER

In this work, we aim to understand the platform-wide requirements to meet the Service Level Objectives (SLOs) of LLMs for different use cases. Platforms are defined as collections of various accelerators connected through an interconnect network, such as Nvidia HGX [26], Google TPU pods [8], Intel HLS-Gaudi2 [17], AMD Instinct MI300X Platform [3], and many more [12], [114] [2], [21], [40].

There is a lack of an existing tool/framework in the community that can help us study LLM inference at various operating points with different inputs. There exist several Neural Processing Unit (NPU) compute simulators [94], [107], [116] but are focused on modeling the compute behavior in detail (e.g., dataflow) and lack support for modeling distributed platforms. Meanwhile, simulators like ASTRA-sim [110] focus on communication optimizations for distributed *training* and do not model the specific prefill-decode pipeline required for distributed *inference*. To address the issue, we build a first-order analytical tool, GenZ². GenZ has three key components: 1) Model Profiler, 2) NPU Characterizer, and 3) Platform Characterizer. We show an overview of GenZ in Fig. 2 and discuss each of its components in the following sections.

A. Target Use Cases

A key difference among LLMs compared to previous DNN models (such as ResNet [74]), is that the model execution shapes vary widely as the use case changes. A *use case* is characterized by three key features :

²<https://github.com/abhibambhaniya/GenZ-LLM-Analyzer>

Real Life Application	# of Tokens Input/Output	Beam Width	TTFT (s)	TPOT (ms)
Question Answering	1000/200	4	0.2	10
Chat Services	3000/1000	2	0.2	10
QA + RAG	10000/200	4	0.4	10
Text Summarization	15000/1000	4	2	20
Code Generation	20000/50	4	0.5	20

TABLE IV: Representative Use Cases of LLM models and their representative input hyperparameters.

- 1) Beam Size, S_b : Number of parallel outputs maintained during the decode phase. Typically value: 2-4.
- 2) Number of Input Tokens, τ_p : Number of tokens that the user has passed as the input prompt. This value varies widely with different applications. T_{TTFT} **depends primarily on** τ_p .
- 3) Number of Output Tokens, τ_d : Number of tokens to be generated during the decode phase in an auto-regressive fashion. Similar to τ_p , this value varies widely with different applications.

Table IV shows the five *use cases* we considered for this work. These have varying input token lengths, output token lengths, and latency constraints. These use cases represent different real-world applications, such as chat Services, code generation, summarization, and question-answering. Additionally, Retrieval augmented generation (RAG) [72], [97] is used in almost all question-answering-based LLM agents. We also model this as a separate use case where the input tokens have context appended to the input prompt.

We use the term LLM *workload* to refer to the specific job running on the hardware platform and placing specific computational demands, and define it as follows:

$Workload = \{U_{seccase}, LLMModel, Optimizations\}$
where

$Optimizations = \{BatchSize, Precision, Parallelism\}$

We use various hugging face datasets [14] along with LLaMA tokenizer [122] to estimate input and output tokens for various use cases. We use dolphin dataset [4] for chat services token estimation. We use LongBench [46] for average token estimation for text summarization [32], [34], [35], [37] and code generation [33], [36]. For RAG-based applications, the context length can vary from a few thousand tokens to tens of thousands of tokens. We use MLDR [55], a Multilingual Long-Document Retrieval dataset built on Wikipedia, to estimate additional context tokens to user input.

B. Model Profiler

Table I shows the details of various LLMs that we study in this work. We consider five different models that serve as a representative set of current state-of-the-art LLMs. We choose models representing the complete spectrum of model size ranging from 7B to 1.8T parameter LLMs. We also have models with different architectures, including MoE-based LLMs (Mixtral-8x7B and GPT4). LLaMA2, LLaMA3, Mixtral, and GPT3 architecture are available openly. We represent GPT4 as a 1.8T parameter mixture-of-experts model, with 120 layers [9], [10], [41]. A single layer of GPT4 has 16 experts

of 111B parameters each, and two experts are activated for each token. There are 55B shared parameters for attention. Each forward pass inference (generation of 1 token) utilizes about 280B parameters and about 560 TFLOPs. A dense 1.8 trillion parameter model would need about 3,700 TFLOP for each inference. We also develop a futuristic Super-LLM model using a scaled-up MoE model, *super LLM*. There are 32 experts per layer and about 10T parameters in total. It is a 128-layer deep model with 4 expert activations per token.

For each new model, GenZ uses the huggingface AutoModels [16] to determine the exact shape of each operator in the model. Since all layers in the LLM are identical, we only need to save the operator dimension of one layer. All LLMs' layer dimensions can be modeled using a few variables, as shown in Table I. Using these stored variables, we calculate the TFLOPS, weight size, KV Cache Estimation, and metrics like arithmetic intensity.

Storing these model operators offline allows us to profile larger context lengths for any LLM model quickly. For example, LLaMA2-7B [123] has a context length limit of 4K [123], but using this offline modeling, we can extend the context length to any size.

We also model popular optimizations in this stage of model profiling, including Kernel Fusion (Flash Attention [60], [61], FLAT [87], Segment KV Caching [128]) and model quantization (FP16, INT8/FP8, INT4/FP4). Since this work focuses on LLM inference, we use INT8 model quantization for all our experiments and results unless specified otherwise.

When profiling MoE models on GenZ, for decode, we assume that irrespective of batch size, only 'k' experts are selected at each layer of each decoding step. In Table I, we indicate the value of 'k' as the experts selected in the last column. For Prefill, we assume that all experts would be activated due to the large number of tokens, irrespective of batch size.

C. NPU Characterizer

Our smallest hardware unit is the accelerator (alternatively referred to as NPU), as shown in Fig. 2. We assume each NPU has a certain amount of efficient compute cores, which can perform $FLOPS$ number of operations per second. In an effort to keep the design space limited, we assume the on-chip memory is enough to achieve maximum computing efficiency. Additionally, we incorporate a computing efficiency factor to account for inefficiencies caused by software and memory synchronization issues.

Each NPU provides access to two external memories (fast and slow). Faster (smaller) memory could be something like an HBM/DDR Memory Bank, while Slower (Larger) memory could be PCIe-accessible CPU memory or CXL-accessible SSD/Flash. Most model weights and activations would prioritize using the Faster memory, however, if the capacity is not enough, data could be potentially offloaded to slower memory. While this would drastically reduce the inference performance, it would still enable inference rather than issuing an out-of-memory (OOM) error.

For the system, we analyze the model performance on an operator-by-operator basis. We follow a roofline-based approach to calculate each operator’s runtime on the accelerator.

$$T_{mem} = \max\left(\frac{\min(M_{op}, S_{fast})}{BW_{fast} \times Eff_{fmem}}, \frac{M_{op} - S_{fast}}{BW_{slow} \times Eff_{smem}}\right) \quad (1)$$

$$T_{op} = \max\left(\frac{C_{op}}{FLOPS \times Eff_C}, T_{mem}\right) \quad (2)$$

S_{fast} is a partition of fast memory allocated to each operator. If $M_{op} > S_{fast}$, the additional data of the operator would be offloaded to the slower memory. Since all parameters, model weights, and KV cache are used uniformly, a fixed portion of the parameters will be offloaded. Using an ideal prefetching scheduler, each operator’s time to read from slower memory could be overlapped with the memory fetches from high-speed memory. Thus, total memory read time would be as shown in Equation 1.

D. Platform Characterizer

We define an inference platform as multiple NPUs connected using an interconnection network (ICN) as shown in Fig. 2. An ICN can have different topological connections, link latencies and varying link bandwidth. Typically distributed LLMs are served using five different types of parallelism strategies, Data Parallel (DP), Tensor parallel (TP) [120], Pipeline parallel (PP) [78], Expert parallel (EP) [65] (Only for MoE models) and Sequence parallel (SP) [81], [99] (primarily for training long sequence).

For TP LLM, an all-reduce communication primitive is required twice per layer. Thus a total of $2 \times$ number of layers all-reduce calls would be made per forward pass of the LLM.

We model all-reduce communication as explained in [44], [110], [127]. For all-reduce of message size M , where M is each accelerator’s initial/final data size, and N is the number of accelerators among which the model is distributed in a tensor parallel fashion. Each accelerator sends M/N -sized data to $N-1$ neighboring accelerators. All-Reduces time is modeled as:

$$T_{AR} = T_{Warmup} + 2(N-1)\left(T_{Link} + \frac{M/N}{BW_{link}Eff_{link}}\right) \quad (3)$$

$$T_{N2N} = T_{Warmup} + T_{Link} + \frac{M}{BW_{link}Eff_{link}} \quad (4)$$

For PP distribution of LLMs, only node-to-node message passing is required. In this case, the time to transfer a message of size M is defined as T_{N2N} .

For EP, two all-to-all would be required among all the nodes, which share experts of a layer. SP requires all gather and reduce scatter per layer.

In our modeling, we have a knob to decide whether to overlap collectives with compute tasks or execute them sequentially. Coordinating the simultaneous execution of collective communication and operator computation is an open

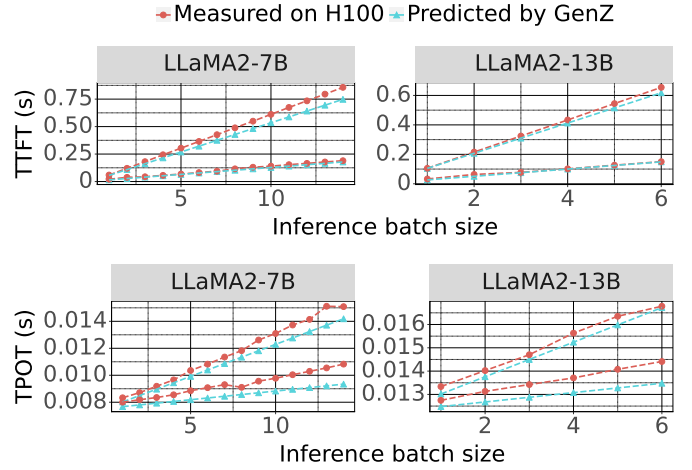


Fig. 4: Comparing GenZ LLM inference modeling against vLLM inference. We vary the input batch size for LLaMA2-7B and LLaMA2-13B on H100 with different input prompt sizes and different LLM models. Different lines represent different input prompt sizes in each graph.

research challenge [108]. Since existing SOTA LLM inference serving frameworks [28], [95], [105] do not incorporate these techniques, we opted to model the interconnect collective communication as non-overlapping. Considering everything, model execution time is defined by (6).

$$T_{layer} = \sum_{Ops} T_{op} + 2T_{AR} \quad (5)$$

$$T_{model} = Layers \times T_{layer} + (PP - 1) \times T_{N2N} \quad (6)$$

E. Validation Studies for GenZ

We validate GenZ on a real hardware platform: A HGX [26] box with 8 NVIDIA H100 SXM GPUs (80 GB) fully connected by NVLinks. We conduct two types of studies: (i) Trends of prefill and decode on a single accelerator system to validate the accelerator modeling by GenZ. (ii) Collective times with different platform sizes to validate the platform interconnect modeling.

Single accelerator platform validation: For the first study, we serve LLaMA2-7B and LLaMA2-13B models using vLLM [96] framework on a H100 GPU. For each model, we run 2 use-cases ($S_b = 1, \tau_p = 544, \tau_d = 200$) and ($S_b = 1, \tau_p = 2173, \tau_d = 200$) and get LLM serving metrics (TTFT, TPOT). We compare this to profiling results generated by GenZ. Since the aim of GenZ is to give first-order analysis, we plug-in empirically measured efficiency factors of 60% for the GPU Tensor TFLOPs and 70% for GPU memory bandwidth. Fig. 4 shows both models’ TTFT and TPOT time comparisons. There is a 5.88% and 3.86% geomean error for TTFT and TPOT between real values and modeled values. This confirms that the trends produced by GenZ align with those observed on actual hardware.

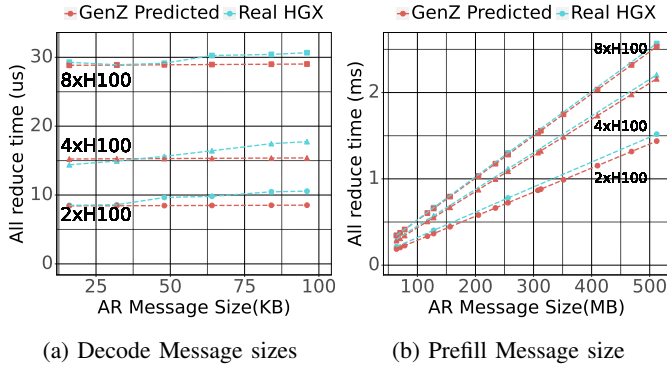


Fig. 5: Comparing All Reduce NCCL latency from GenZ against HGX:8xH100 box. Platform sizes of 2, 4, and 8 GPUs for varying message sizes.

Platform interconnect validation: To verify the collectives time at platform scale, we benchmark all-reduce communication primitive with `nccl-tests` [24], a communication primitive performance benchmark for NVIDIA GPUs. GenZ’s collective communication times are validated with a platform size of 2 GPUs, 4 GPUs, and 8 GPUs. For collective communications, we observed an average link efficiency of 75% for NVLINK, which gives an effective link BW of 350 GB/s for each GPU in HGX box. We profile all combinations of use case (Table IV) and model (Table I) and collect their all-reduce (AR) message sizes. The message size of each AR call is very small (< 128 KB) for decode, while for prefill, per call message size is a few hundred MBs. Fig. 5 compares the real hardware latency for three different platform sizes and the corresponding latency generated by GenZ. Since the prefill and decode stages have stark differences in message size, we verify the collective time for prefill and decode independently. We found that for decode message sizes, the link latency, T_{Link} is the dominating, thus the latency seems almost constant. While prefill AR messages are large enough, that the link bandwidth, BW_{Link} , is the main contributor to collective time. Collective for all datapoints, there is a 3.89% and 2.7% geomean error for decode and prefill message sizes between real values and GenZ values.

V. WORKLOAD OPTIMIZATION ANALYSIS WITH GENZ

For LLM inference, batch size, precision, and parallelism are considered optimizations aimed at improving performance, efficiency, and resource utilization without modifying the core implementation of the LLM. It’s important to note that while these optimizations can improve inference performance, some of them may also introduce trade-offs or limitations. For example, lower precision may result in some loss of accuracy, while parallelism strategies can introduce communication overhead or require specialized hardware configurations. In this section, we study the effect of input batching and parallelization strategies on LLM inference.

A. Input Batching

Since most of the operators in the decode phase are memory-bound, batching multiple queries can help in im-

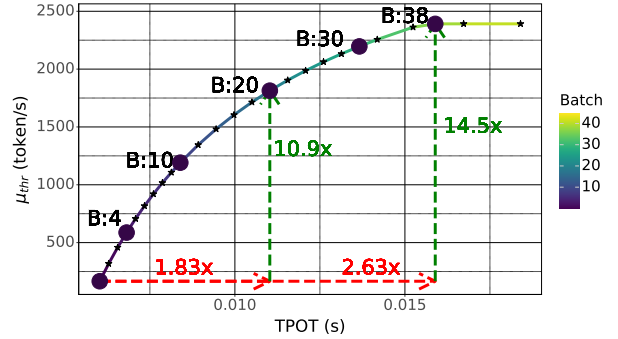


Fig. 6: Impact of batching on decode throughput and TPOT.

proving the decode throughput. Fig. 6 shows how the μ_{thr} and TPOT increase with increase in batch size. Running a LLaMA2-7B model at int8 precision on NVIDIA’s A100 (80GB) GPU, with 2k input tokens, as we increase the batch from 1 to 44, we see a 10.9 \times improvement in the μ_{thr} while TPOT only increasing by 1.83 \times . The μ_{thr} becomes constant after $B = 38$. After this point, the decode latency increases linearly with batch size. The saturated throughput is 14.5 times the $B=1$ throughput with only 2.63 \times increase in latency. Thus, *batching inputs during the decoding phase proves to be highly advantageous.*

Static batching [15], [25] and continuous batching [43], [76], [95], [130] represent the two primary batching mechanisms commonly employed for LLM serving. In static batching, all available requests are batched together, but all the forward passes for these requests are completed before any other requests are run. A key challenge with static batching is higher queuing latency for new requests. For continuous batching, new queries can be added after each forward pass. The prefill stage of the new queries can be run along with the decode phase of the older queries. Thus, it helps reduce the queuing time for new queries but can result in higher tail latency for initial queries. In this work, we gain our insights primarily from static batching, but these insights would work for platforms running continuous batching as well.

B. Parallelization Strategies

Meeting SLO demands another reason to scale up the number of accelerators in the platform. However, there is a lack of clarity about the impact of the parallelism strategy. An optimal parallelization strategy may vary depending on the model and workload configuration. We also observe drastic contrast in how different parallelization strategies work during the prefill and decode stage. Fig. 7 shows the example of how model weights and KV cache split with different degrees of TP + PP. We restrict our evaluations to TP and PP in this work across the diverse LLMs. We leave platform implications of EP and SP for MoEs as future work.

Fig. 8 compares different LLM models on HGX: H100x8. We use a workload with $S_b = 4$, $\tau_p = 4000$, $\tau_d = 256$.

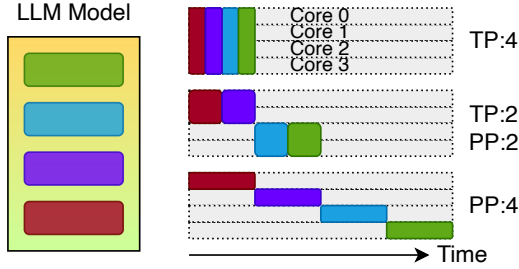


Fig. 7: Various parallelization strategies. Each grey box represents an accelerator NPUs and the colored blocks represent the layers. We illustrate how the LLM runs on different NPUs for each strategy. (a) In full TP weights of all layers are equally distributed among all NPUs. (b) With hybrid TP and PP, the layers are distributed among groups of accelerators. Within a group, the layer weights are distributed in tensor parallel fashion. (c) Full PP splits all layers across the NPUs. In all cases, once the model has been partitioned via TP/PP, DP is employed across the remaining NPUs in the platform.

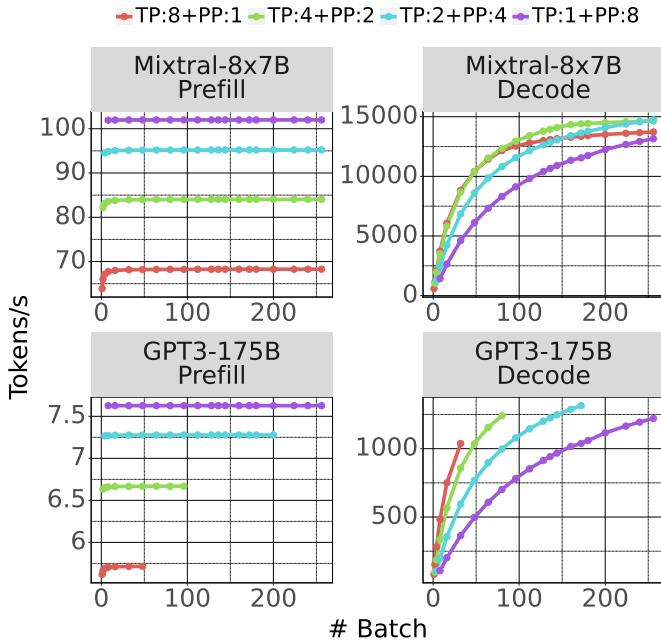


Fig. 8: Comparing different parallelism strategies for LLM inference on HGX:H00x8.

Key takeaways for choosing parallelization strategy:

- **Prefill:** PP can serve many more queries than TP. PP=8 can 2.32x, 1.38x more query compared to TP=8 for Mixtral 8x7B and GPT3-175B.
- **Decode:** TP only or Mixture of TP + PP is generally superior for throughput. On the other hand, higher PP enables the platform to accommodate much higher batch sizes. For example, HGX:H100x8 with PP=8 can accommodate GPT3-175B, which can accommodate a batch size of 256 due to micro-batching, while TP gives an OOM error after B=32.

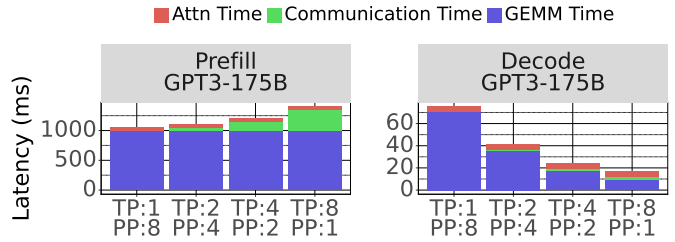


Fig. 9: GPT3 runtime breakdown for various parallelism strategies on HGX: H100x8.

We show runtime breakdown in Fig. 9 to understand these performance gains. We ran GPT3-175B with batch size 8, beam size 4, and 4000 input tokens and 256 output tokens. In the compute-bound prefill phase, the compute of all NPUs is fully saturated, and thus, GEMM and SA times remain constant, irrespective of micro-batch size. The differentiating factor is the *collective times*. TP:8 requires two ARs for each layer, thus a total of 192 collectives with 8 NPUs. Meanwhile, PP:8 all needs to send messages at the interface of pipeline stages, thus only 7 collectives. In the memory-bound decode phase, we see a contrasting behavior. Due to the very small AR message size, the collective time remains small. Having smaller micro-batch sizes with PP further reduces collective time. With PP, serialized execution of layers results in larger latency. It should be noted that while total latency would be higher, per-stage latency would be reduced as PP goes down.

VI. PLATFORM CHARACTERISTICS ANALYSIS WITH GENZ

In this section, we use GenZ to study different platform characteristics. We explore four key platform characteristics: TFLOPS (HW_c), Memory BW (BW_{fast}), Interconnect link bandwidth (BW_{link}), Interconnect link latency (T_{Link}) To understand the effect of each characteristic on LLM inference performance, we vary each parameter keeping everything else constant. We assume an NPU with 800 TFLOPS, 40 GB HBM memory @ 4000 GB/s memory bandwidth, 300 GB/s interconnect bandwidth, and link latency of 2 us. For each parameter, we study all use cases in Table IV and all models in Table I, but in the interest of space we only show a few key data points in the main text.

A. TFLOPS Scaling

We vary the platform TFLOPS by 2x, 4x, 8x, 12x. We show Mixtral 8x7B and GPT-3 inference on platforms with 2 and 12 NPUs, respectively. We chose RAG-based question answering as the representative use case of the study. Fig. 10 shows the runtime breakdown for the prefill and decode stage. We observe 4.33x and 2x reduction in prefill latency going 12x the original compute TFLOPS. For GPT3-175B, we see a smaller improvement in TTFT latency as it is dominated by the communication time, but the increased FLOPS would only reduce the prefill and attention time.

- Increasing computation has the potential to reduce the prefill latency significantly, but there is no impact on the decoding latency.
- **The benefits from increasing FLOPS diminish as platform size grows due to the significant contribution of network latency in prefill.**

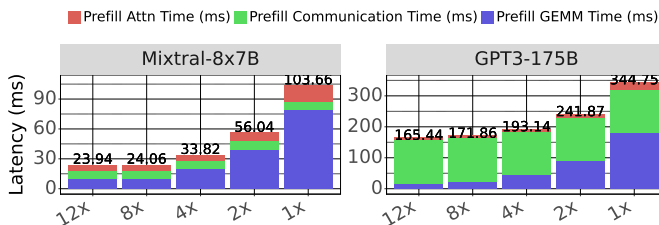
B. Memory Bandwidth Scaling

We vary the platform memory bandwidth by $2\times$, $4\times$, $8\times$, $12\times$. We show Mixtral 8x7B and GPT-3 inference on the platform with 2 and 12 NPUs, respectively. We chose text summarization as the representative use case for the study. Fig. 11 shows the runtime breakdown for the prefill and decode stage. We observe $4.21\times$ and $1.73\times$ reduction in decode latency when going to $8\times$ the original compute memory BW. Similar to TFLOPS scaling, we see a smaller improvement in decode latency when it is dominated by the communication time.

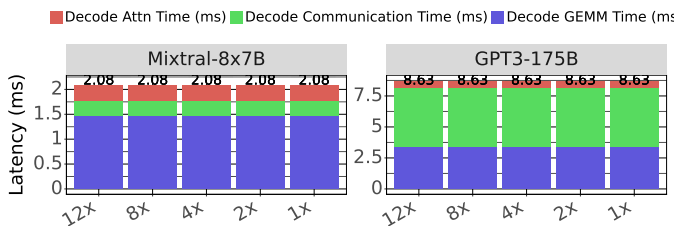
- Increasing bandwidth has the potential to reduce the decoding latency significantly, but there is no impact on the prefill latency.
- **Like in TFLOPS, the benefits from increasing fast memory bandwidth diminish as platform size grows, owing to the substantial impact of network latency during decoding.**

C. ICN BW

Next, we vary the platform interconnect network bandwidth by $1\times$, $2\times$, $3\times$, $6\times$. We show GPT3-175B and GPT4-175B inference on the platform with 24 and 84 NPUs, respectively. We chose code generation as the representative use case of this study. Fig. 12 shows the runtime breakdown for the prefill and decode stages. We observe $1.44\times$ and $1.56\times$ reduction in prefill latency as ICN BW is increased to $6\times$ the original BW.

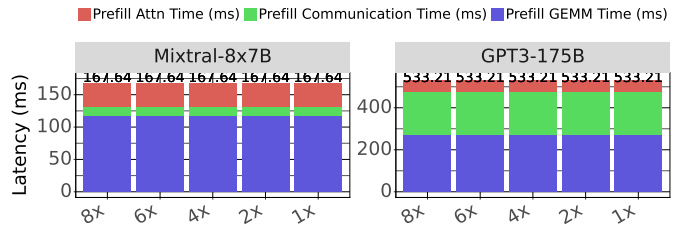


(a) Prefill ✓

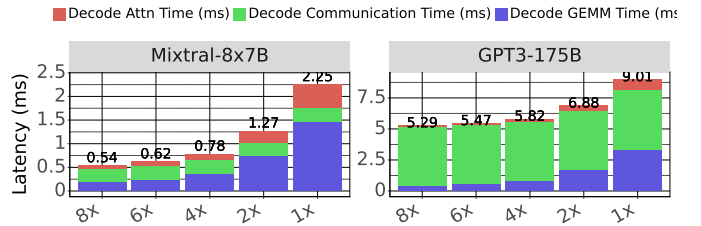


(b) Decode ✗

Fig. 10: Scaling TFLOPS for various models on Rag-based question answering use case. Mixtral requires only 2 accelerators. GPT3 uses 12 accelerators with TP:12.

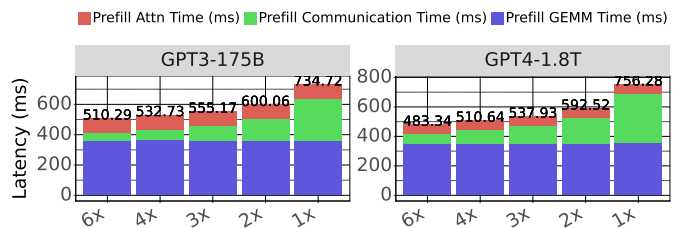


(a) Prefill ✗

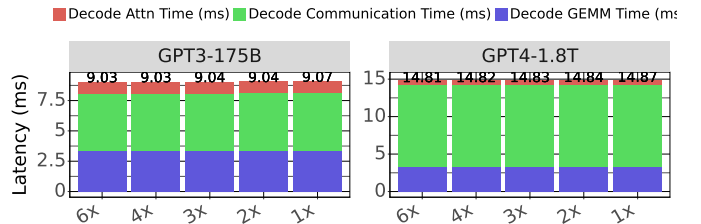


(b) Decode ✓

Fig. 11: Scaling Memory bandwidth per accelerator for text summarization use case. Mixtral requires only 2 accelerators. GPT3 uses 12 accelerators with TP:12.



(a) Prefill ✓



(b) Decode ✗

Fig. 12: Scaling interconnect network BW for platform running code-generation use case. GPT3 and GPT4 uses 24(TP:12+PP:2) and 84(TP:21+PP:4) NPUs respectively.

- Increasing ICN BW has the potential to reduce the prefill latency significantly, but there is minimal impact on the decoding latency.
- **The benefits from increasing interconnect network bandwidth are only visible when platform size is significant such that network latency is in prefill.**

D. ICN Link Latency

Finally, to study the impact of platform interconnect network link latency, we reduce the T_{link} remove 2 us to 0.1 us. GPT3-175B and GPT4-175B inference on the platform with

24 and 84 NPUs, respectively. We choose code generation as the representative use case of this study. Fig. 13 shows the runtime breakdown for the prefill and decode stage. We observe a 1.8x and 2.9x reduction in the decoding latency as T_{link} goes from 2 us to 0.1 us.

Our interconnect network modeling for the platform assumes the optimal topology for linking accelerators. Delving into different topologies for LLM inference presents a vast design space and currently a topic of research [127].

- Reducing interconnect network latency reduces the decode latency significantly, but there minimal impact on the prefill latency.
- **The benefits from reducing interconnect network link latency are only visible when platform sizes are of a significant size such that network latency is in decode.**

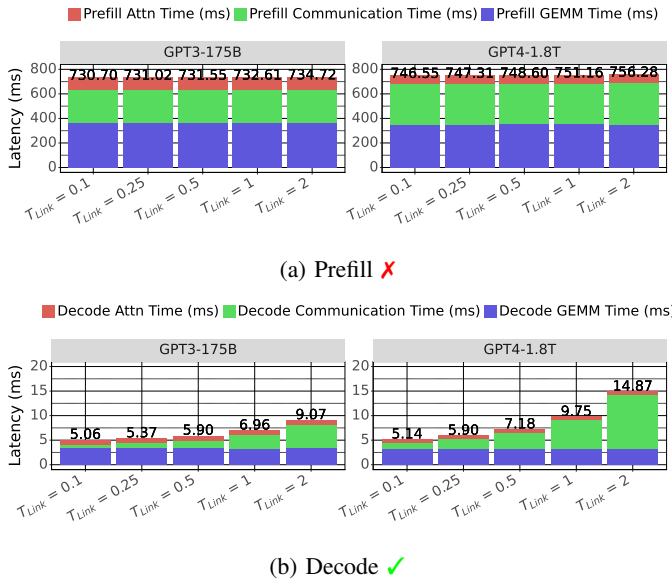


Fig. 13: Scaling Interconnect network link latency for a model with code-generation use case. GPT3 uses 24 accelerators with TP:12+PP:2, and GPT4 uses 84 accelerators with TP:21+PP:4.

E. Fewer Chips with offload.

The most effective approach for serving inference involves storing all model weights and key-value (KV) cache in the fast memory of the NPU, such as HBM. However, this may not always be feasible due to resource limitations. In such cases, the model weights and KV cache can be transferred to slower memory. For LLM inference, where both model weights and KV cache are utilized simultaneously, a viable strategy is to offload a fixed portion of model weights and KV cache. Illustrated in Fig. 14 shows profiling of LLaMA3-70B with parameters $S_b = 4, \tau_p = 8000, \tau_d = 256$ on platforms equipped with 2 and 4 A100-40GB GPUs (PCIe) and consequences of employing an offload-based system for LLM inference are depicted. While the model fits on the platform at smaller batch sizes, an increase in batch size leads

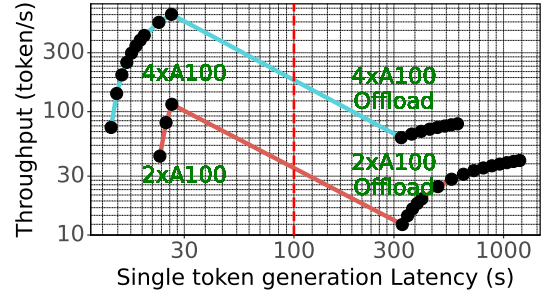


Fig. 14: Running LLaMA3-70B with some parameters offloaded to slower memory via the host. All points on the right side of the red line of the plot have offloaded parameters.

to greater KV cache requirements, resulting in the offloading of some parameters. Consequently, inference latency rises by 13.2x and 12.7x due to offloading for 2xA100 and 4xA100 configurations, respectively. Thus offloading parameters can ensure correctness, but comes with a heavy penalty in the inference performance.

VII. PLATFORM REQUIREMENTS ESTIMATION WITH GENZ

In this section, we answer the question that **given a LLM use case, what should be the platform configuration to meet the SLO requirements?** Prefill and decode phase presents its own set of unique platform requirements. The key platform requirements terms are computation operations (PetaFLOPs), memory bandwidth (TB/s), and memory capacity (GBs). These metrics are crucial for understanding the hardware resources needed to run LLM models on various workloads efficiently. These requirements are dictated by *workload*. Our aim is to quantify these requirements and provide analytical equations to scale the requirements. We study each of the three requirements in isolation by assuming the rest of the components are not the bottleneck for the use case and model.

A. Platform Memory Capacity Requirement

For LLM inference on the platform, there should be enough memory capacity to store complete model parameters + KV cache in the fast memory of NPUs. Where $KV\ cache = 2 * B * (\tau_p + S_b * \tau_d) * H_{kv} * D/H * N_{layers}$.

Figure 15 illustrates the distribution of memory requirements across various models and usage scenarios. For LLaMA2-7B, LLaMA3-70B, and GPT3-175B, all model parameters are utilized in each inference iteration, whereas in Mixtral-8x7B and GPT4-1.8T, only 27% and 15% of the total model parameters are activated per inference cycle.

As model sizes increase, the ratio of KV cache parameters to active weights diminishes progressively. Specifically, the ratio of the largest KV cache size (Code Gen) to active weights is 82%, 11%, 20%, 27%, and 2.8% for LLaMA2-7B, Mixtral-8x7B, LLaMA2-70B, GPT3-175B, and GPT4-1.8T, respectively. Moreover, MoE models exhibit significantly smaller KV caches compared to dense LLMs. Additionally, it is noteworthy that the KV cache expands linearly with

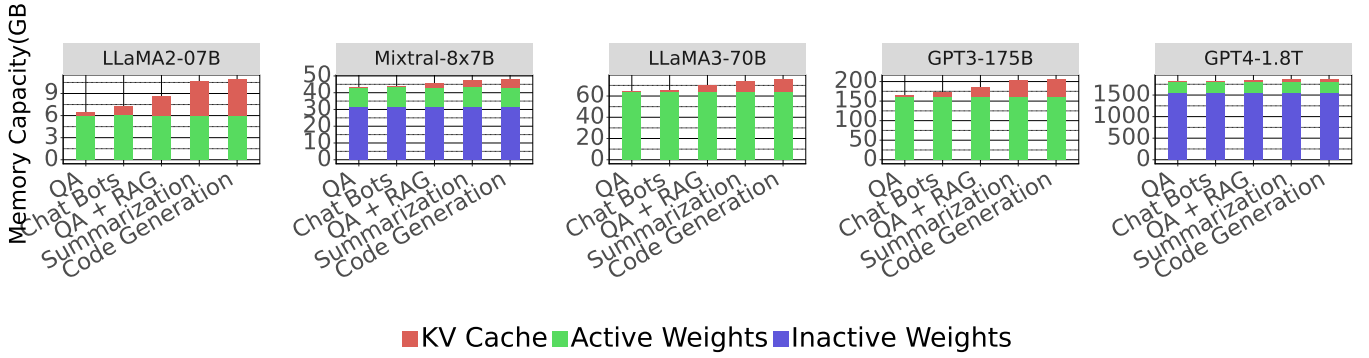


Fig. 15: Memory Capacity (GB) required for various models on different use cases during the decode stage.

the batch size. Furthermore, Mixtral 8x7B and LLaMA3-70VB employ GQA to minimize the KV cache footprint, thus enhancing batch size capabilities.

Key Takeaways:

- ISO-usecase, $MEM-CAP_{Req} \propto O(ModelSize + KV\ cache)$.
- ISO-model, $MEM-CAP_{Req} \propto O(B * (\tau_p + S_b * \tau_d))$.

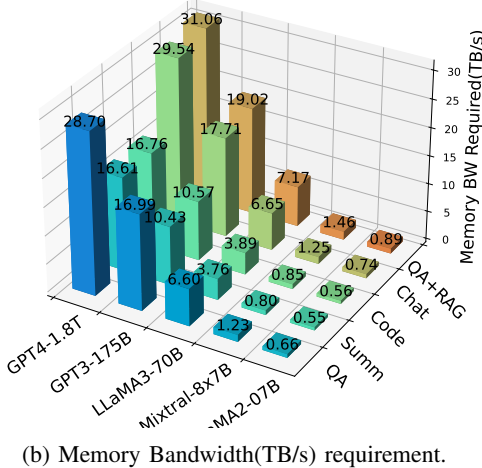
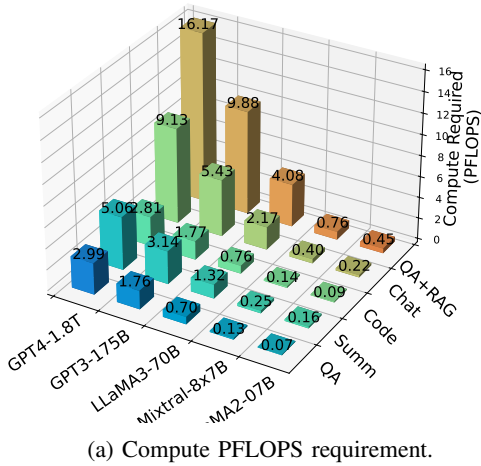


Fig. 16: Platform Scale requirements.

B. Platform Compute Requirement

Given that the prefill stage is predominantly compute-bound, the platform prerequisites for TFLOPs are determined by prefill stage across all scenarios. Fig. 16(a) shows the platform-level compute TFLOPs required to meet the requirements in Table IV for various models.

The compute TFLOPS is contingent upon both the model's dimensions and the quantity of input tokens. In cases where there are lenient expectations regarding Time to First Token (TTFT), the required TFLOPS also decreases. When using RAG for question answering, the increased prompt size causes the TFLOPS requirement to go up by 5.41x across all models.

Key Takeaways:

- ISO-usecase, $TFLOPS_{Req} \propto O(\frac{ModelSize + KV\ cache}{TTFT})$.
- ISO-model, $TFLOPS_{Req} \propto O(\frac{B * \tau_p}{TTFT})$.

C. Platform Memory Bandwidth Requirement

The memory bandwidth required to satisfy TPOT constraints dictates the platform requirements. Fig. 16(b) shows the platform level memory BW required to meet the requirements for various workloads. We assume the LLM inference with model weights and KV cache in FP8 format. Changing the dataformat would proportionally scale up or down the bandwidth requirements. For GPT4, the memory bandwidth going from QA to RAG based QA only increased the requirement by 8% even with context length becoming 10x. This is owing to the large size of the model itself.

Key Takeaways:

- ISO-usecase, $BW_{Req} \propto O(\frac{Active\ Model + KV\ cache}{TPOT})$.
- ISO-model, $BW_{Req} \propto O(\frac{B * (\tau_p + S_b * \tau_d)}{TPOT})$.

VIII. EXTREME SCALE REQUIREMENTS: AI ASSISTANT

Examining the trajectory of model scaling over the past couple of years suggests an ongoing trend of increasing model size [29]. Moreover, there has been a steady rise in the maximum context lengths of large language models (LLMs). [27]. For instance, the GPT-4-Prompts dataset, comprising multi-turn conversational prompts, already features prompts of up to 900k tokens. [23]. Recently introduced, Google Gemini can accommodate prompts of up to 1M tokens in production [69]. In this section, we delineate the platform requirements

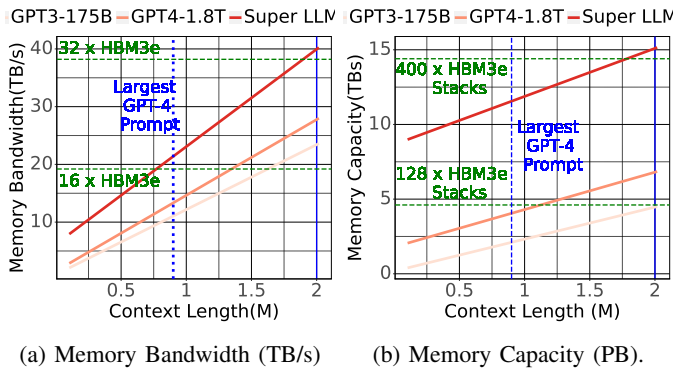


Fig. 17: Platform Scale requirements supporting a real-time conversational AI personal assistant.

for serving these forthcoming LLMs with extensive context lengths and juxtapose them with the current state-of-the-art standards.

We envision an enormous 10T parameter Super-LLM model as the futuristic model from Table I. Our aim is to employ the Super-LLM as a standard AI assistant capable of engaging in **real-time conversations with humans**, furnishing answers on diverse topics, and retaining recollections of past interactions. Hence, supporting large context windows is imperative for AI assistants. This workload can be characterized as $S_b = 4$, $\tau_p = \text{Variable}$, $\tau_d = 2000$. Given its role as a personal assistant, we would operate it with a batch size of 1. For seamless conversation, we assume it can generate output at the rate at which humans read or listen, which amounts to 300 words per minute [51].

For real-time conversations, the KV cache would grow linearly with context, leading to higher memory capacity and bandwidth requirements. Fig. 17 shows the memory bandwidth and capacity required for using the super LLM as context lengths scale to 2M tokens. To gauge its feasibility, we compare it against the current SOTA memory, HBM3e, with 1.2TB/s BW and 36 GB memory capacity per stack. We require 40 TB/s memory bandwidth to make a super-LLM AI assistant, which equates to roughly 32 HBM3e stacks. On the other hand, it would require around 15 TB of memory capacity, equating to 400 HBM3e stacks.

Key Takeaway:

- The platform memory capacity seems to be a more intensive bottleneck than the memory bandwidth.
- Memory BW is within a reasonable range due to the sparse activation of the model. The growth of memory capacity requirement seems unsustainable.

IX. RELATED WORKS

LLM inference serving and analysis. We are seeing a massive uprising works related to LLM inference serving. There are works on optimizing the batching [43], [76], [130], memory optimization [61], [95] and scheduling [67], [119]. Various articles [1], [6], [7], [13], [18], [19], [38] provides

metrics, analysis, insights, and best practices for LLM inference performance on current hardware systems. Various works provided a survey [58], [90], [131] of transformer inference and various optimizations in existing transformer architecture on current hardware systems.

HW for LLM inference and Hardware Modeling. Chiplet Cloud [109] is a chiplet-based ASIC AI supercomputer architecture that optimizes total cost of ownership (TCO) per generated token for serving large generative language models. LLMCompass [132] does DSE for LLM in its framework models the details of NPU architecture. There has been a lot of work in DNN inference design-space modeling [62], [63], [94], [98], [101], [107], [113], [117] which focus on modeling latency, bandwidth, and energy efficiency of various dataflows and loop ordering. Apart from compute modeling, network simulators like ASTRA-sim [111], [126] model communication in distributed training.

X. CONCLUSION

With the recent advancement of LLMs, designing HW platform for efficient LLM serving becomes crucial to provide high throughput with low latency while maintaining cost-efficiency. To understand the implication of HW platform requirements for LLM inference considering diverse models, use cases, and SLO, we introduce GenZ, a first-order analytical tool. Using GenZ, we conduct three main analyses: 1) An analysis of the performance impact of different workload optimization, 2) An analysis of the performance impact of different platform characterizations, and 3) An analysis of the platform requirements for the target LLM inference with the target use case and SLO. We believe our proposed tool and analyses would shed light on future platform designs for next-generation HWs and LLMs.

REFERENCES

- [1] “Accelerating self-attentions for llm serving with flashinfer.” [Online]. Available: <https://flashinfer.ai/2024/02/02/introduce-flashinfer.html>
- [2] “Amazon web services.” [Online]. Available: <https://aws.amazon.com>
- [3] “Amd instinct mi300x plat- form.” [Online]. Available: <https://www.amd.com/en/products/accelerators/instinct/mi300.html#case-studies>
- [4] “Cognitivecomputations dolphin model, hugging face.” [Online]. Available: <https://huggingface.co/cognitivecomputations/dolphin-2.6-mixtral-8x7b>
- [5] “Dbrx, a large language model by databricks.” [Online]. Available: <https://github.com/databricks/dbrx>
- [6] “Dissecting batching effects in gpt inference.” [Online]. Available: <https://le.qun.ch/en/blog/2023/05/13/transformer-batching/>
- [7] “Generative llm inference with neuron.” [Online]. Available: <https://awsdocs-neuron.readthedocs-hosted.com/en/latest/general/appnotes/transformers-neuronx/generative-llm-inference-with-neuron.html#what-batch-size-should-i-use>
- [8] “Google tpu pods.” [Online]. Available: <https://cloud.google.com/blog/topics/tpus/google-showcases-cloud-tpu-v4-pods-for-large-model-training>
- [9] “Gpt-4 architecture details.” [Online]. Available: <https://patmccguinness.substack.com/p/gpt-4-details-revealed>
- [10] “Gpt-4 architecture, infrastructure, training dataset, costs, vision, moe.” [Online]. Available: <https://www.semianalysis.com/p/gpt-4-architecture-infrastructure>
- [11] “Grok-1.” [Online]. Available: <https://github.com/xai-org/grok-1>
- [12] “Groqchip.” [Online]. Available: <https://groq.com/wp-content/uploads/2022/10/GroqChip-Processor-Product-Brief-v1.5.pdf>

- [13] “A guide to llm inference and performance.” [Online]. Available: <https://www.baseten.co/blog/llm-transformer-inference-guide/>
- [14] “Hugging face datasets.” [Online]. Available: <https://huggingface.co/datasets>
- [15] “Hugging face pipelines.” [Online]. Available: https://huggingface.co/docs/transformers/en/main_classes/pipelines
- [16] “Huggingface generate infereface.” [Online]. Available: https://huggingface.co/docs/transformers/en/main_classes/text_generation
- [17] “Intel hls-gaudi2.” [Online]. Available: https://habana.ai/wp-content/uploads/2023/10/HLS-Gaudi2_Datasheet_10_23.pdf
- [18] “Llm inference performance engineering: Best practices.” [Online]. Available: <https://www.databricks.com/blog/llm-inference-performance-engineering-best-practices>
- [19] “Mastering llm techniques: Inference optimization.” [Online]. Available: <https://developer.nvidia.com/blog/mastering-llm-techniques-inference-optimization/>
- [20] “Meta llama 3.” [Online]. Available: <https://github.com/meta-llama/llama3>
- [21] “Microsoft azure.” [Online]. Available: <https://azure.microsoft.com/en-us>
- [22] “Mixtral-8x22b.” [Online]. Available: <https://huggingface.co/mistral-community/Mixtral-8x22B-v0.1>
- [23] “Multi-turn conversational prompts from chatgpt-4 (10k+ tokens).” [Online]. Available: <https://huggingface.co/datasets/erfanzar/GPT-4-Prompts>
- [24] “Nccl tests.” [Online]. Available: <https://github.com/NVIDIA/nccl-tests/tree/master>
- [25] “Nvidia faster transformer.” [Online]. Available: <https://github.com/NVIDIA/FasterTransformer>
- [26] “Nvidia hgx.” [Online]. Available: <https://www.nvidia.com/en-us/data-center/hgx/>
- [27] “Openai’s plans according to sam altman.” [Online]. Available: <https://web.archive.org/web/20230601163710/https://humanloop.com/blog/openai-plans>
- [28] “Rayllm - llms on ray.” [Online]. Available: <https://github.com/ray-project/ray-llm>
- [29] “The rise and rise of a.i. large language models (llms).” [Online]. Available: <https://informationisbeautiful.net/visualizations/the-rise-of-generative-ai-large-language-models-llms-like-chatgpt/>
- [30] “Sora.” [Online]. Available: <https://openai.com/sora>
- [31] “Text generation inference.” [Online]. Available: <https://github.com/huggingface/text-generation-inference>
- [32] “Thudm longbench govreport dataset, hugging face.” [Online]. Available: <https://huggingface.co/datasets/THUDM/LongBench/viewer/Govreport>
- [33] “Thudm longbench lcc dataset, hugging face.” [Online]. Available: <https://huggingface.co/datasets/THUDM/LongBench/viewer/LCC>
- [34] “Thudm longbench multinews dataset, hugging face.” [Online]. Available: <https://huggingface.co/datasets/THUDM/LongBench/viewer/multinews>
- [35] “Thudm longbench qmsum dataset, hugging face.” [Online]. Available: <https://huggingface.co/datasets/THUDM/LongBench/viewer/QMSum>
- [36] “Thudm longbench repobench-p dataset, hugging face.” [Online]. Available: <https://huggingface.co/datasets/THUDM/LongBench/viewer/RepoBench-P>
- [37] “Thudm longbench vcsun dataset, hugging face.” [Online]. Available: <https://huggingface.co/datasets/THUDM/LongBench/viewer/VCSUM>
- [38] “Transformer inference arithmetic.” [Online]. Available: <https://kipp.ly/transformer-inference-arithmetic/>
- [39] “Triton tensorrt-llm backend.” [Online]. Available: https://github.com/triton-inference-server/tensorrtllm_backend
- [40] “Sambanova whitepaper,” 2021. [Online]. Available: https://sambanova.ai/wp-content/uploads/2021/06/SambaNova_RDA_Whitepaper_English.pdf
- [41] J. Achiam, S. Adler, S. Agarwal, L. Ahmad, I. Akkaya, F. L. Aleman, D. Almeida, J. Altenschmidt, S. Altman, S. Anadkat *et al.*, “Gpt-4 technical report,” *arXiv preprint arXiv:2303.08774*, 2023.
- [42] M. Agarwal, A. Qureshi, N. Sardana, L. Li, J. Quevedo, and D. Khudia, “Llm inference performance engineering: Best practices,” Oct 2023. [Online]. Available: <https://www.databricks.com/blog/llm-inference-performance-engineering-best-practices>
- [43] A. Agrawal, A. Panwar, J. Mohan, N. Kwatra, B. S. Gulavani, and R. Ramjee, “Sarathi: Efficient llm inference by piggybacking decodes with chunked prefills,” *arXiv preprint arXiv:2308.16369*, 2023.
- [44] A. Alexandrov, M. F. Ionescu, K. E. Schauer, and C. Scheiman, “Loggp: Incorporating long messages into the logp model for parallel computation,” *Journal of Parallel and Distributed Computing*, vol. 44, no. 1, pp. 71–79, 1997. [Online]. Available: <https://www.sciencedirect.com/science/article/pii/S0743731597913460>
- [45] Anthropic, “Claude.” [Online]. Available: <https://www.anthropic.com/claude>
- [46] Y. Bai, X. Lv, J. Zhang, H. Lyu, J. Tang, Z. Huang, Z. Du, X. Liu, A. Zeng, L. Hou, Y. Dong, J. Tang, and J. Li, “Longbench: A bilingual, multitask benchmark for long context understanding,” *arXiv preprint arXiv:2308.14508*, 2023.
- [47] A. R. Bambhaniya, A. Yazdanbakhsh, S. Subramanian, S.-C. Kao, S. Agrawal, U. Evci, and T. Krishna, “Progressive gradient flow for robust n:m sparsity training in transformers,” 2024.
- [48] S. Borgeaud, A. Mensch, J. Hoffmann, T. Cai, E. Rutherford, K. Millican, G. B. Van Den Driessche, J.-B. Lespiau, B. Damoc, A. Clark *et al.*, “Improving language models by retrieving from trillions of tokens,” in *International conference on machine learning*. PMLR, 2022, pp. 2206–2240.
- [49] N. Brandes, D. Ofer, Y. Peleg, N. Rappoport, and M. Linial, “Proteinbert: a universal deep-learning model of protein sequence and function,” *Bioinformatics*, vol. 38, pp. 2102–2110, 4 2022. [Online]. Available: https://github.com/nadavbra/protein_bert
- [50] T. Brown, B. Mann, N. Ryder, M. Subbiah, J. D. Kaplan, P. Dhariwal, A. Neelakantan, P. Shyam, G. Sastry, A. Askell *et al.*, “Language models are few-shot learners,” *Advances in neural information processing systems*, vol. 33, pp. 1877–1901, 2020.
- [51] M. Brysbaert, “How many words do we read per minute? a review and meta-analysis of reading rate,” *Journal of Memory and Language*, vol. 109, p. 104047, 2019. [Online]. Available: <https://www.sciencedirect.com/science/article/pii/S0749596X19300786>
- [52] E. Caballero, K. Gupta, I. Rish, and D. Krueger, “Broken neural scaling laws,” 2023.
- [53] M. Cao, Y. Dong, J. Wu, and J. C. K. Cheung, “Factual error correction for abstractive summarization models,” in *Proceedings of the 2020 Conference on Empirical Methods in Natural Language Processing (EMNLP)*. Association for Computational Linguistics, 2020, p. undefined.
- [54] Chatgpt, “Introducing chatgpt.” [Online]. Available: <https://openai.com/blog/chatgpt>
- [55] J. Chen, S. Xiao, P. Zhang, K. Luo, D. Lian, and Z. Liu, “Bge m3-embedding: Multi-lingual, multi-functionality, multi-granularity text embeddings through self-knowledge distillation,” 2024.
- [56] J. Chen, H. Lin, X. Han, and L. Sun, “Benchmarking large language models in retrieval-augmented generation,” in *Proceedings of the AAAI Conference on Artificial Intelligence*, vol. 38, no. 16, 2024, pp. 17754–17762.
- [57] Y. Chen, X. Pan, Y. Li, B. Ding, and J. Zhou, “Ee-llm: Large-scale training and inference of early-exit large language models with 3d parallelism,” *arXiv preprint arXiv:2312.04916*, 2023.
- [58] K. T. Chitty-Venkata, S. Mittal, M. Emani, V. Vishwanath, and A. K. Somani, “A survey of techniques for optimizing transformer inference,” 2023.
- [59] A. Chowdhery, S. Narang, J. Devlin, M. Bosma, G. Mishra, A. Roberts, P. Barham, H. W. Chung, C. Sutton, S. Gehrmann *et al.*, “Palm: Scaling language modeling with pathways,” *arXiv preprint arXiv:2204.02311*, 2022.
- [60] R. Dao, “Flash-decoding for long-context inference.” [Online]. Available: <https://pytorch.org/blog/flash-decoding/>
- [61] T. Dao, D. Y. Fu, S. Ermon, A. Rudra, and C. Ré, “Flashattention: Fast and memory-efficient exact attention with io-awareness,” 2022.
- [62] S. Dave, Y. Kim, S. Avancha, K. Lee, and A. Shrivastava, “Dmazerunner: Executing perfectly nested loops on dataflow accelerators,” *ACM Transactions on Embedded Computing Systems (TECS)*, vol. 18, no. 5s, pp. 1–27, 2019.
- [63] S. Dave, A. Shrivastava, Y. Kim, S. Avancha, and K. Lee, “dmazerunner: Optimizing convolutions on dataflow accelerators,” in *ICASSP 2020-2020 IEEE International Conference on Acoustics, Speech and Signal Processing (ICASSP)*. IEEE, 2020, pp. 1544–1548.
- [64] M. Elbayad, J. Gu, E. Grave, and M. Auli, “Depth-adaptive transformer,” *arXiv preprint arXiv:1910.10073*, 2019.
- [65] W. Fedus, B. Zoph, and N. Shazeer, “Switch transformers: Scaling to trillion parameter models with simple and efficient sparsity,” *arXiv preprint arXiv:2101.03961*, 2021.

- [66] E. Frantar and D. Alistarh, "Sparsegpt: Massive language models can be accurately pruned in one-shot," in *International Conference on Machine Learning*. PMLR, 2023, pp. 10323–10337.
- [67] Y. Fu, P. Bailis, I. Stoica, and H. Zhang, "Break the sequential dependency of llm inference using lookahead decoding," *arXiv preprint arXiv:2402.02057*, 2024.
- [68] A. Gholami, S. Kim, Z. Dong, Z. Yao, M. W. Mahoney, and K. Keutzer, "A survey of quantization methods for efficient neural network inference," in *Low-Power Computer Vision*. Chapman and Hall/CRC, 2022, pp. 291–326.
- [69] Google, "Introducing gemini: Google's most capable ai model yet." [Online]. Available: <https://blog.google/technology/ai/google-gemini-ai/>
- [70] J. Gou, B. Yu, S. J. Maybank, and D. Tao, "Knowledge distillation: A survey," *International Journal of Computer Vision*, vol. 129, no. 6, pp. 1789–1819, 2021.
- [71] N. M. Guerreiro, D. M. Alves, J. Waldendorf, B. Haddow, A. Birch, P. Colombo, and A. F. Martins, "Hallucinations in large multilingual translation models," *Transactions of the Association for Computational Linguistics*, vol. 11, pp. 1500–1517, 2023.
- [72] K. Guu, K. Lee, Z. Tung, P. Pasupat, and M. Chang, "Retrieval augmented language model pre-training," in *International conference on machine learning*. PMLR, 2020, pp. 3929–3938.
- [73] H. He, H. Zhang, and D. Roth, "Rethinking with retrieval: Faithful large language model inference," *arXiv preprint arXiv:2301.00303*, 2022.
- [74] K. He, X. Zhang, S. Ren, and J. Sun, "Deep residual learning for image recognition," in *2016 IEEE Conference on Computer Vision and Pattern Recognition (CVPR)*, 2016, pp. 770–778.
- [75] G. Hinton, O. Vinyals, and J. Dean, "Distilling the knowledge in a neural network," *arXiv preprint arXiv:1503.02531*, 2015.
- [76] C. Holmes, M. Tanaka, M. Wyatt, A. A. Awan, J. Rasley, S. Rajbhandari, R. Y. Aminabadi, H. Qin, A. Bakhtiari, L. Kurilenko *et al.*, "DeepSpeed-fastgen: High-throughput text generation for llms via mii and DeepSpeed-inference," *arXiv preprint arXiv:2401.08671*, 2024.
- [77] A. Holtzman, J. Buys, L. Du, M. Forbes, and Y. Choi, "The curious case of neural text degeneration," 2020.
- [78] Y. Huang, Y. Cheng, A. Bapna, O. Firat, M. X. Chen, D. Chen, H. Lee, J. Ngiam, Q. V. Le, Y. Wu, and Z. Chen, "Gpipe: Efficient training of giant neural networks using pipeline parallelism," 2019.
- [79] HyunSeobKim, "Chem-bert: Molecular representation learning." [Online]. Available: <https://github.com/HyunSeobKim/CHEM-BERT>
- [80] G. Izacard, P. Lewis, M. Lomeli, L. Hosseini, F. Petroni, T. Schick, J. Dwivedi-Yu, A. Joulin, S. Riedel, and E. Grave, "Atlas: Few-shot learning with retrieval augmented language models," *Journal of Machine Learning Research*, vol. 24, no. 251, pp. 1–43, 2023.
- [81] S. A. Jacobs, M. Tanaka, C. Zhang, M. Zhang, S. L. Song, S. Rajbhandari, and Y. He, "DeepSpeed-ulysses: System optimizations for enabling training of extreme long sequence transformer models," 2023.
- [82] H. Jegou, M. Douze, and C. Schmid, "Product quantization for nearest neighbor search," *IEEE transactions on pattern analysis and machine intelligence*, vol. 33, no. 1, pp. 117–128, 2010.
- [83] G. Jeong, P.-A. Tsai, A. R. Bambhaniya, S. W. Keckler, and T. Krishna, "Abstracting sparse dnn acceleration via structured sparse tensor decomposition," 2024.
- [84] Z. Ji, N. Lee, R. Frieske, T. Yu, D. Su, Y. Xu, E. Ishii, Y. J. Bang, A. Madotto, and P. Fung, "Survey of hallucination in natural language generation," *ACM Computing Surveys*, vol. 55, no. 12, pp. 1–38, 2023.
- [85] A. Q. Jiang, A. Sablayrolles, A. Roux, A. Mensch, B. Savary, C. Bamford, D. S. Chaplot, D. d. l. Casas, E. B. Hanna, F. Bressand *et al.*, "Mixtral of experts," *arXiv preprint arXiv:2401.04088*, 2024.
- [86] H. Kang, Q. Zhang, S. Kundu, G. Jeong, Z. Liu, T. Krishna, and T. Zhao, "Gear: An efficient kv cache compression recipe for near-lossless generative inference of llm," 2024.
- [87] S.-C. Kao, S. Subramanian, G. Agrawal, and T. Krishna, "An optimized dataflow for mitigating attention performance bottlenecks," *arXiv preprint arXiv:2107.06419*, 2021.
- [88] J. Kaplan, S. McCandlish, T. Henighan, T. B. Brown, B. Chess, R. Child, S. Gray, A. Radford, J. Wu, and D. Amodei, "Scaling laws for neural language models," 2020.
- [89] C. W. Kim, "Guiding text generation with constrained beam search in transformers," Mar 2022. [Online]. Available: <https://huggingface.co/blog/constrained-beam-search>
- [90] S. Kim, C. Hooper, T. Wattanawong, M. Kang, R. Yan, H. Genc, G. Dinh, Q. Huang, K. Keutzer, M. W. Mahoney *et al.*, "Full stack optimization of transformer inference: a survey," *arXiv preprint arXiv:2302.14017*, 2023.
- [91] S. Kim, K. Mangalam, S. Moon, J. Malik, M. W. Mahoney, A. Gholami, and K. Keutzer, "Speculative decoding with big little decoder," *Advances in Neural Information Processing Systems*, vol. 36, 2024.
- [92] N. Kishore Kumar and J. Schneider, "Literature survey on low rank approximation of matrices," *Linear and Multilinear Algebra*, vol. 65, no. 11, pp. 2212–2244, 2017.
- [93] D. Kondratyuk, L. Yu, X. Gu, J. Lezama, J. Huang, G. Schindler, R. Hornung, V. Birodkar, J. Yan, M.-C. Chiu, K. Somandepalli, H. Akbari, Y. Alon, Y. Cheng, J. Dillon, A. Gupta, M. Hahn, A. Hauth, D. Hendon, A. Martinez, D. Minnen, M. Sirotenko, K. Sohn, X. Yang, H. Adam, M.-H. Yang, I. Essa, H. Wang, D. A. Ross, B. Seybold, and L. Jiang, "Videopoet: A large language model for zero-shot video generation," 2024.
- [94] H. Kwon, P. Chatarasi, V. Sarkar, T. Krishna, M. Pellauer, and A. Parashar, "Maestro: A data-centric approach to understand reuse, performance, and hardware cost of dnn mappings," *IEEE Micro*, vol. 40, no. 3, pp. 20–29, 2020.
- [95] W. Kwon, Z. Li, S. Zhuang, Y. Sheng, L. Zheng, C. H. Yu, J. Gonzalez, H. Zhang, and I. Stoica, "Efficient memory management for large language model serving with pagedattention," in *Proceedings of the 29th Symposium on Operating Systems Principles*, ser. SOSP '23. New York, NY, USA: Association for Computing Machinery, 2023, p. 611–626. [Online]. Available: <https://doi.org/10.1145/3600006.3613165>
- [96] W. Kwon, Z. Li, S. Zhuang, Y. Sheng, L. Zheng, C. H. Yu, J. E. Gonzalez, H. Zhang, and I. Stoica, "Efficient memory management for large language model serving with pagedattention," in *Proceedings of the ACM SIGOPS 29th Symposium on Operating Systems Principles*, 2023.
- [97] P. Lewis, E. Perez, A. Piktus, F. Petroni, V. Karpukhin, N. Goyal, H. Küttler, M. Lewis, W.-t. Yih, T. Rocktäschel *et al.*, "Retrieval-augmented generation for knowledge-intensive nlp tasks," *Advances in Neural Information Processing Systems*, vol. 33, pp. 9459–9474, 2020.
- [98] R. Li, Y. Xu, A. Sukumaran-Rajam, A. Rountev, and P. Sadayappan, "Analytical characterization and design space exploration for optimization of cnns," in *Proceedings of the 26th ACM International Conference on Architectural Support for Programming Languages and Operating Systems*, 2021, pp. 928–942.
- [99] S. Li, F. Xue, C. Baranwal, Y. Li, and Y. You, "Sequence parallelism: Long sequence training from system perspective," 2022.
- [100] X. Li, X. Zhu, Z. Ma, X. Liu, and S. Shah, "Are chatgpt and gpt-4 general-purpose solvers for financial text analytics? an examination on several typical tasks," *arXiv preprint arXiv:2305.05862*, 2023.
- [101] W. Lu, G. Yan, J. Li, S. Gong, Y. Han, and X. Li, "Flexflow: A flexible dataflow accelerator architecture for convolutional neural networks," in *2017 IEEE International Symposium on High Performance Computer Architecture (HPCA)*. IEEE, 2017, pp. 553–564.
- [102] Y. A. Malkov and D. A. Yashunin, "Efficient and robust approximate nearest neighbor search using hierarchical navigable small world graphs," *IEEE transactions on pattern analysis and machine intelligence*, vol. 42, no. 4, pp. 824–836, 2018.
- [103] C. Meister, T. Vieira, and R. Cotterell, "Best-first beam search," 2022.
- [104] Microsoft, "Github copilot · your ai pair programmer." [Online]. Available: <https://github.com/features/copilot>
- [105] NVIDIA, "Nvidia. tensorrt-llm." [Online]. Available: <https://github.com/NVIDIA/TensorRT-LLM>
- [106] H. Ootomo, A. Naruse, C. Nolet, R. Wang, T. Feher, and Y. Wang, "Cagra: Highly parallel graph construction and approximate nearest neighbor search for gpus," *arXiv preprint arXiv:2308.15136*, 2023.
- [107] A. Parashar, P. Raina, Y. S. Shao, Y.-H. Chen, V. A. Ying, A. Mukkara, R. Venkatesan, B. Khailany, S. W. Keckler, and J. Emer, "Timeloop: A systematic approach to dnn accelerator evaluation," in *2019 IEEE International Symposium on Performance Analysis of Systems and Software (ISPASS)*, 2019, pp. 304–315.
- [108] P. Patel, E. Choukse, C. Zhang, Íñigo Goiri, A. Shah, S. Maleki, and R. Bianchini, "Splitwise: Efficient generative llm inference using phase splitting," 2023.
- [109] H. Peng, S. Davidson, R. Shi, S. L. Song, and M. Taylor, "Chiplet cloud: Building ai supercomputers for serving large generative language models," 2023.
- [110] S. Rashidi, S. Sridharan, S. Srinivasan, and T. Krishna, "ASTRA-SIM: Enabling sw/hw co-design exploration for distributed dl training

- platforms,” in *IEEE International Symposium on Performance Analysis of Systems and Software (ISPASS)*, 2020.
- [111] S. Rashidi, S. Sridharan, S. Srinivasan, and T. Krishna, “Astrsim: Enabling sw/hw co-design exploration for distributed dl training platforms,” in *2020 IEEE International Symposium on Performance Analysis of Systems and Software (ISPASS)*. IEEE, 2020, pp. 81–92.
- [112] V. Raunak, A. Menezes, and M. Junczys-Dowmunt, “The curious case of hallucinations in neural machine translation,” in *Proceedings of the 2021 Conference of the North American Chapter of the Association for Computational Linguistics: Human Language Technologies*, 2021, pp. 1172–1183.
- [113] B. Reagen, J. M. Hernández-Lobato, R. Adolf, M. Gelbart, P. Whatmough, G.-Y. Wei, and D. Brooks, “A case for efficient accelerator design space exploration via bayesian optimization,” in *2017 IEEE/ACM International Symposium on Low Power Electronics and Design (ISLPED)*. IEEE, 2017, pp. 1–6.
- [114] K. Rocki, D. Van Essendelft, I. Sharapov, R. Schreiber, M. Morrison, V. Kibardin, A. Portnoy, J. F. Dietiker, M. Syamlal, and M. James, “Fast stencil-code computation on a wafer-scale processor,” in *SC20: International Conference for High Performance Computing, Networking, Storage and Analysis*. IEEE, 2020, pp. 1–14.
- [115] E. Roivainen, “I gave chatgpt an iq test. here’s what i discovered — scientific american.” [Online]. Available: <https://www.scientificamerican.com/article/i-gave-chatgpt-an-iq-test-heres-what-i-discovered/>
- [116] A. Samajdar, J. M. Joseph, Y. Zhu, P. Whatmough, M. Mattina, and T. Krishna, “A systematic methodology for characterizing scalability of dnn accelerators using scale-sim,” in *2020 IEEE International Symposium on Performance Analysis of Systems and Software (ISPASS)*, 2020, pp. 58–68.
- [117] A. Samajdar, J. M. Joseph, Y. Zhu, P. Whatmough, M. Mattina, and T. Krishna, “A systematic methodology for characterizing scalability of dnn accelerators using scale-sim,” in *2020 IEEE International Symposium on Performance Analysis of Systems and Software (ISPASS)*. IEEE, 2020, pp. 58–68.
- [118] X. Shen, Z. Chen, M. Backes, and Y. Zhang, “In chatgpt we trust? measuring and characterizing the reliability of chatgpt,” *arXiv preprint arXiv:2304.08979*, 2023.
- [119] Y. Sheng, L. Zheng, B. Yuan, Z. Li, M. Ryabinin, D. Y. Fu, Z. Xie, B. Chen, C. Barrett, J. E. Gonzalez, P. Liang, C. Ré, I. Stoica, and C. Zhang, “Flexgen: High-throughput generative inference of large language models with a single gpu,” 2023.
- [120] M. Shoenybi, M. Patwary, R. Puri, P. LeGresley, J. Casper, and B. Catanzaro, “Megatron-lm: Training multi-billion parameter language models using model parallelism,” *arXiv preprint arXiv:1909.08053*, 2019.
- [121] H. Sun, X. Liu, Y. Gong, Y. Zhang, D. Jiang, L. Yang, and N. Duan, “Allies: Prompting large language model with beam search,” 2023.
- [122] H. Touvron, T. Lavril, G. Izacard, X. Martinet, M.-A. Lachaux, T. Lacroix, B. Rozière, N. Goyal, E. Hambro, F. Azhar, A. Rodriguez, A. Joulin, E. Grave, and G. Lample, “Llama: Open and efficient foundation language models,” 2023.
- [123] H. Touvron, L. Martin, K. Stone, P. Albert, A. Almahairi, Y. Babaei, N. Bashlykov, S. Batra, P. Bhargava, S. Bhosale *et al.*, “Llama 2: Open foundation and fine-tuned chat models,” *arXiv preprint arXiv:2307.09288*, 2023.
- [124] A. Vaswani, N. Shazeer, N. Parmar, J. Uszkoreit, L. Jones, A. N. Gomez, Ł. Kaiser, and I. Polosukhin, “Attention is all you need,” *Advances in neural information processing systems*, vol. 30, 2017.
- [125] J. Wei, Y. Tay, R. Bommasani, C. Raffel, B. Zoph, S. Borgeaud, D. Yogatama, M. Bosma, D. Zhou, D. Metzler, E. H. Chi, T. Hashimoto, O. Vinyals, P. Liang, J. Dean, and W. Fedus, “Emergent abilities of large language models,” 2022.
- [126] W. Won, T. Heo, S. Rashidi, S. Sridharan, S. Srinivasan, and T. Krishna, “Astra-sim2. 0: Modeling hierarchical networks and disaggregated systems for large-model training at scale,” in *2023 IEEE International Symposium on Performance Analysis of Systems and Software (ISPASS)*. IEEE, 2023, pp. 283–294.
- [127] W. Won, S. Rashidi, S. Srinivasan, and T. Krishna, “Exploring multi-dimensional hierarchical network topologies for efficient distributed training of trillion parameter dl models,” 2021.
- [128] H. Wu, Y. Gan, F. Yuan, J. Ma, W. Zhu, Y. Xu, H. Zhu, Y. Zhu, X. Liu, and J. Gu, “Efficient llm inference solution on intel gpu,” 2023.
- [129] G. Xiao, J. Lin, M. Sez nec, H. Wu, J. Demouth, and S. Han, “Smoothquant: Accurate and efficient post-training quantization for large language models,” 2023.
- [130] G.-I. Yu, J. S. Jeong, G.-W. Kim, S. Kim, and B.-G. Chun, “Orca: A distributed serving system for {Transformer-Based} generative models,” in *16th USENIX Symposium on Operating Systems Design and Implementation (OSDI 22)*, 2022, pp. 521–538.
- [131] Z. Yuan, Y. Shang, Y. Zhou, Z. Dong, Z. Zhou, C. Xue, B. Wu, Z. Li, Q. Gu, Y. J. Lee, Y. Yan, B. Chen, G. Sun, and K. Keutzer, “Llm inference unveiled: Survey and roofline model insights,” 2024.
- [132] H. Zhang, A. Ning, R. Prabhakar, and D. Wentzlaff, “A hardware evaluation framework for large language model inference,” *arXiv preprint arXiv:2312.03134*, 2023.
- [133] W. X. Zhao, K. Zhou, J. Li, T. Tang, X. Wang, Y. Hou, Y. Min, B. Zhang, Z. Zhang, Z. Dong, Y. Du, C. Yang, Y. Chen, Z. Chen, J. Jiang, R. Ren, Y. Li, X. Tang, Z. Liu, P. Liu, J.-Y. Nie, and J.-R. Wen, “A survey of large language models,” 2023.
- [134] W. Zhao, S. Tan, and P. Li, “Song: Approximate nearest neighbor search on gpu,” in *2020 IEEE 36th International Conference on Data Engineering (ICDE)*. IEEE, 2020, pp. 1033–1044.